Carbon Nanodots

International Edition: DOI: 10.1002/anie.201510158
German Edition: DOI: 10.1002/ange.201510158

Synthesis, Separation, and Characterization of Small and Highly Fluorescent Nitrogen-Doped Carbon NanoDots

Francesca Arcudi, Luka Đorđević, and Maurizio Prato**

Dedicated to Professor Giacinto Scoles on the occasion of his 80th birthday

Abstract: *A facile bottom-up approach to carbon nanodots (CNDs) is reported, using a microwave-assisted procedure under controlled conditions. The as-prepared nitrogen-doped CNDs (NCNDs) show narrow size-distribution, abundant surface traps and functional groups, resulting in tunable fluorescent emission and excellent solubility in water. Moreover, we present a general method for the separation of NCNDs by low-pressure size-exclusion chromatography, leading to an even narrower size distribution, different surface composition, and optical properties. They display among the smallest size and the highest FLQYs reported so far. ^{13}C-enriched starting materials produced N^{13}CNDs suitable for thorough NMR studies, which gave useful information on their molecular structure. Moreover, they can be easily functionalized and can be used as water-soluble carriers. This work provides an avenue to size- and surface-controllable and structurally defined NCNDs for applications in areas such as optoelectronics, biomedicine, and bioimaging.*

Extensive effort has been devoted to obtain non-toxic fluorescent nanomaterials as an alternative to the popular semiconductor-based quantum dots (QDs). Carbon nanodots (CNDs) are recently discovered nanocarbons that comprise discrete, quasispherical nanoparticles with sizes below 10 nm.[1] CNDs were first discovered during the purification of single-walled carbon nanotubes through preparative electrophoresis in 2004[2] and, owing to their interesting properties, have gradually become a prominent new member of the nanocarbon family.[3–5]

Compared to traditional semiconductor QDs and organic dyes, photoluminescent CNDs are potentially superior in terms of biological properties, high (aqueous) solubility, robust chemical inertness, facile modification, and high resistance to photobleaching.[4,6–8] Their properties give them a high potential in biomedical, optronic, and catalytic applications.[9–17] A very interesting property of CNDs is their tunable emission, characterized by multi-fluorescence (FL) colors under varied excitation wavelengths.

A number of different synthetic procedures have been developed and reported for the preparation of CNDs, usually classified as top-down or bottom-up.[4,16] However, the structure and size of CNDs are still difficult to control. Therefore, a simple and cost-effective process, giving high quality and homogeneous nanodots, remains a challenge.

To improve the fluorescence efficiency of CNDs, two approaches are usually employed and involve surface modification and/or element doping.[1,18,19] Nitrogen doping has been reported to give excellent optical properties and usually blue-shifted fluorescence, although most of the time nitrogen atoms are introduced under harsh conditions.[20–23] Amino acids are ideal carbon and nitrogen sources for CNDs owing to their low cost and abundance.[23,24] Moreover, molecules containing primary amines allow simultaneous nitrogen doping and surface passivation during the synthetic process.[25]

The use of microwaves (MW) is a possible alternative synthetic approach, which would avoid multi-step synthesis and provide benefits from features such as faster rates, milder conditions, and low energy consumption.[25–28]

Herein, we report a simple bottom-up method for highly fluorescent nitrogen-doped CNDs (NCNDs), using a MW reactor under controlled conditions, without the need of sophisticated equipment and/or additional surface passivation. We also report the separation of NCNDs with low-pressure gel permeation chromatography, which results in an effective strategy for quasi-monodispersed NCNDs with improved optical properties. Finally, NMR experiments carried out on ^{13}C-enriched NCNDs allowed us to obtain important structural information.

Arginine (Arg) and ethylenediamine (EDA) were used as carbon and nitrogen sources. The heterogeneous solution underwent thermal carbonization of the precursors and led to nucleation. Finally, the nuclei grew by diffusion of other molecules towards the surface of the nanoparticles. In the process of microwave heating, the solution changed color from transparent to dark brown as a result of the formation of NCNDs (Supporting Information, Figure S1). The MW parameters were optimized to obtain the desired properties of the final material, in terms of optical performance (see below). Appropriate viscosity and temperature control are needed for a uniform carbonization process that leads to the formation of NCNDs. Fluorescent NCNDs were obtained at 240 °C, 26 bar, 200 W with a MW heating time of 180 seconds using water as reaction medium (Supplementary Informa-

[*] F. Arcudi, L. Đorđević, Prof. M. Prato
Department of Chemical and Pharmaceutical Sciences
INSTM UdR Trieste, University of Trieste
Trieste 34127 (Italy)
E-mail: francesca.arcudi@phd.units.it
prato@units.it
Prof. M. Prato
Carbon Nanobiotechnology Laboratory
CIC biomaGUNE, Paseo de Miramón 182
20009 Donostia-San Sebastian (Spain)
Basque Fdn Sci, Ikerbasque, Bilbao 48013, Spain

Supporting information for this article is available on the WWW under http://dx.doi.org/10.1002/anie.201510158.

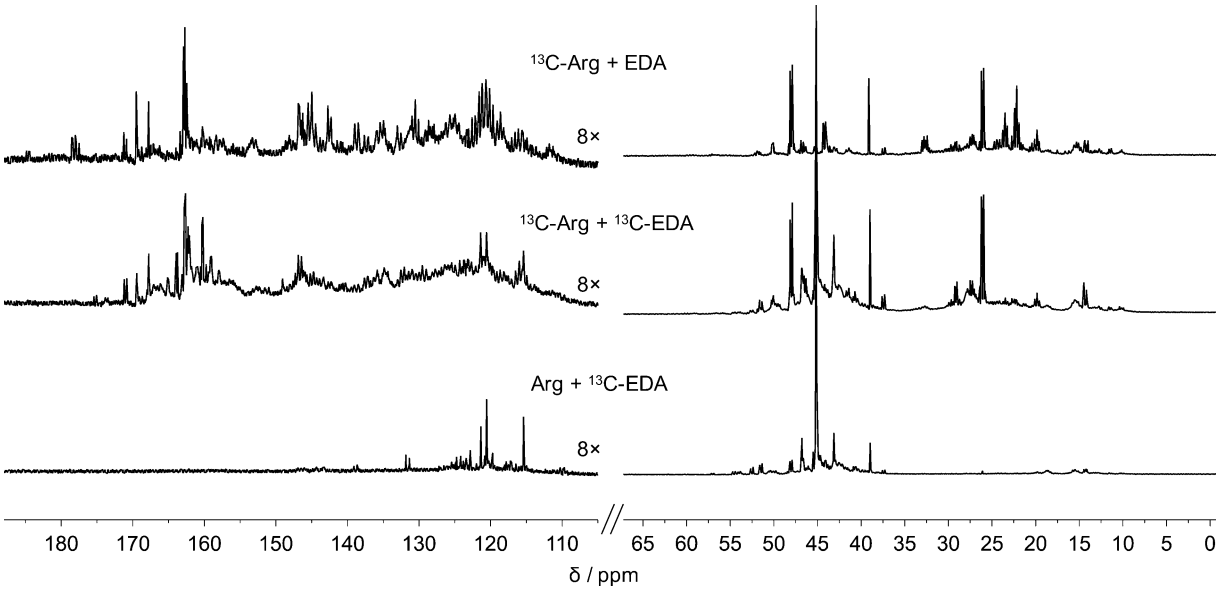

Figure 1. ^{13}C-NMR spectra of N^{13}CNDs prepared starting from ^{13}C-Arg and EDA (top), ^{13}C-Arg and ^{13}C-EDA (middle), and Arg and ^{13}C-EDA (bottom). The intensity of the aromatic region was increased 8.0 times to facilitate the visualization.

tion). Large carbon nanoparticles were removed by filtration and the yellow solution was dialyzed against Milli-Q water. The obtained NCNDs (26% yield based on weight) exhibited a high solubility in water (up to 80 mg mL^{-1}) and also in common polar organic solvents.

To gain unprecedented structural information, we prepared ^{13}C-enriched NCNDs (N^{13}CNDs) for ^{13}C-NMR investigations (Figure 1), starting with fully ^{13}C-enriched Arg and EDA. A tentative interpretation of a representative structural unit of NCNDs is reported in Figure 2, with a very general peak assignment. Typically, ^{13}C-NMR spectra of N^{13}CNDs consist of an aliphatic region (Figure 2, C_a), with carbon atoms connected to heteroatoms (Figure 2, C_b) or to an aromatic core (Figure 2, C_c) and an aromatic region (Figure 2 $C_{d\text{-}h}$). First of all, the contribution of each component was evaluated, using separated and combined ^{13}C-Arg and ^{13}C-EDA (Figure 1; Supporting Information, Figures S3–S6). Figure 1-top shows the ^{13}C-NMR spectrum of NCNDs produced using only ^{13}C-enriched Arg. It is clear that the aromatic core and the aliphatic as well as the carbonyl regions mainly originate from Arg. While EDA mostly contributes to the typical region of aliphatic carbon atoms connected to heteroatoms, signals arising from EDA were also found in the aromatic core of N^{13}CNDs. Further bidimensional experiments (^{1}H-^{13}C) revealed numerous H–C correlations both by direct (HSQC, Figure 2 H_a–C_a H_b–C_b H_c–C_c; Supporting Information, Figures S7–S9) or through multiple-bond correlations (HMBC, Figure 2 H_a–C_b–C_c H_c–C_d–C_e; Supporting Information, Figures S10–S12). Remarkably, protons that lie in the aliphatic region and close to heteroatoms were found to correlate with the aromatic sp^2-carbon core (Figure 2, red lines). Analogous data was obtained from ^{13}C-^{13}C one bond correlation (INADEQUATE, Figure 2 C_a–C_c C_c–C_d C_f–C_g–C_h; Supporting Information, Figures S13–S15). Additionally, diffusion-ordered spectroscopy (DOSY, Figure S16) was performed through ^{1}H–^{13}C multiple-bond correlation to unambiguously assign the signals to macromolecular species. ^{15}N-NMR preliminary experiments were also performed, but they were not as informative as the ^{13}C-NMR spectra (Figure S17). As a provisional conclusion, we can say that our NCNDs are polymeric, rounded-shaped materials, containing both aliphatic and aromatic regions with many amino groups amenable to further functionalization.

Atomic force microscopy (AFM) confirmed the round shape and showed that NCNDs (as-prepared NCNDs, from now on ap-NCNDs) have a rather homogeneous size distribution (Figure 2 a,e,i; Supporting Information, Figure S18). By statistical analysis of the height of about one hundred nanoparticles, we determined an average size of 2.47 ± 0.84 (full width at half-maximum (FWHM): 1.977).

The crude mixture of NCNDs produced after MW treatment was separated by means of low-pressure gel filtration chromatography using a column packed with Sephadex LH-20 and operating at a pressure of 150 psi. According to their elution time, we collected three fractions, named NCNDs **1** (19% yield based on weight), NCNDs **2** (10% yield based on weight), and NCNDs **3** (11% yield based on weight), whose sizes were analyzed by AFM. AFM images, height profiles, and size distributions of the three fractions are reported in Figure 2 b–d,f–h,j–l and Figures S19–21. Average sizes of 2.65 ± 0.48 (FWHM: 1.141), 2.04 ± 0.57 (FWHM: 1.345), and 1.24 ± 0.43 (FWHM: 1.013) were determined for NCNDs **1**, NCNDs **2**, and NCNDs **3**, respectively. These are among the smallest CNDs ever reported.[5,29]

The structure and composition of the ap-NCNDs, as well as the separated NCNDs **1–3,** were determined by FT-IR spectroscopy and X-ray photoelectron spectroscopy (XPS). FT-IR spectrum (Figure 3 a) show that ap-NCNDs have many oxygenated functional groups on their surface, such as carboxylic acid, epoxy, alkoxy, hydroxy, and carbonyl groups. Absorptions at 1194 and 1111 cm^{-1} can be attributed to C–O–C bonds, while absorptions at 1350 and 1318 cm^{-1}

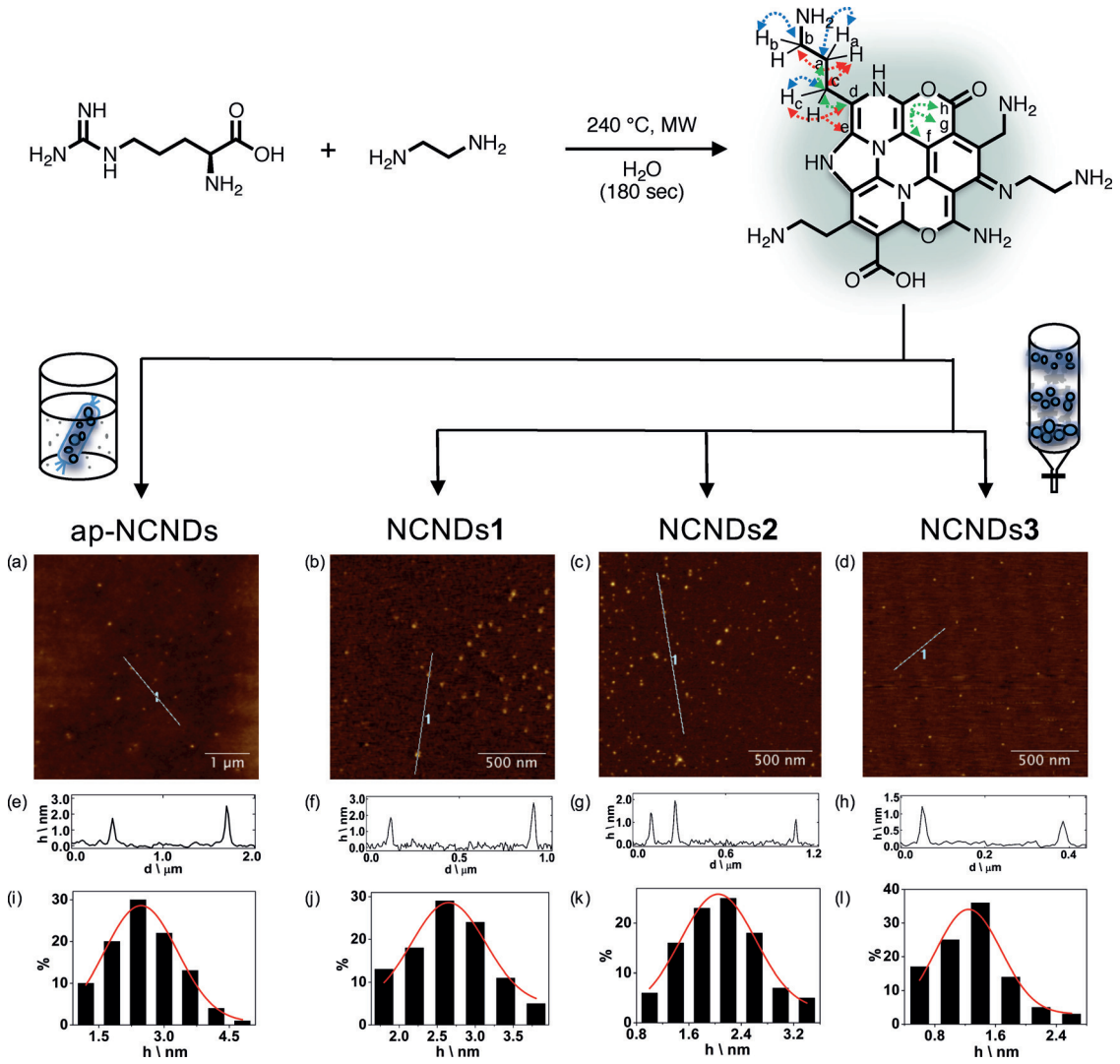

Figure 2. Reaction scheme for NCNDs and their functional groups. Representative structural correlations found in NMR experiments are reported in dashed arrows (HSQC blue lines, HMBC red lines, and INADEQUATE green lines). a–d) Tapping mode AFM images of ap-NCNDs (5.0×5.0 μm) and NCNDs **1**–**3** (1.7×1.7 μm) on a mica substrate; e–h) Height profiles of ap-NCNDs and NCNDs **1**–**3**; i–l) Size histograms of ap-NCNDs and NCNDs **1**–**3** with curves fit to the data using a Gaussian model.

confirm the presence of C–O bonds. Moreover, the absorption peaks at 1655, 1704, and 1767 cm^{-1} are indicative of C=O bonds, whereas the broad peak centered at 3299 cm^{-1} revealed O–H/N–H bonding. Furthermore, C–N (1492 and 1437 cm^{-1}) and C=N (1557 cm^{-1}) functional groups can be identified, while peaks at 2932 and 2862 cm^{-1} are related to the C–H bond stretching vibrations.

The separated NCNDs **1**, NCNDs **2**, and NCNDs **3** have similar IR spectra, suggesting a similar functional groups distribution (Figure S22). To further confirm the functional groups present on the surface of NCNDs, XPS characterization was carried out. From the full-scan XPS spectrum of ap-NCNDs (Figure 3b) C, N, and O are detected with peaks at 286.8 eV (C1s), 400.33 eV (N1s), and 532.34 eV (O1s) respectively. To determine the C and N configurations in the ap-NCNDs, C1s and N1s spectra were analyzed (Figure 3c,d). The XPS spectrum of C1s can be deconvoluted into five surface components corresponding to sp^2(C=C) at 284.5 eV, sp^3 (C–C, and C–H) at 285.5 eV, C–O/C–N at 286.2 eV, C=O/C=N at 288.3 eV, as well as COOH at 290.5 eV. The N1s spectrum can be deconvoluted into four peaks centered at 398.3, 399.6, 400.5, and 401.9 eV corresponding to C=N, NH_2, C–N–C and N–C_3 respectively.[21,22,30] The surface components of ap-NCNDs, as determined by XPS, are in good agreement with the FT-IR and NMR results. The presence of primary amino groups was confirmed by a positive Kaiser test. From this highly sensitive colorimetric test, it was possible to estimate a value of 1350 μmol g^{-1} of amino groups: their presence allows easy insertion of further functional groups and/or interesting molecules/ions through standard organic chemistry procedures.[28] As an example of post-functionalization with interesting moieties, we prepared the NCNDs-porphyrin conjugate **2** (Scheme 1).

The amino groups of the NCNDs were coupled with the carboxylic acid functionalized porphyrin **1** (Scheme S1). The resulting conjugate was found to be highly soluble in water,

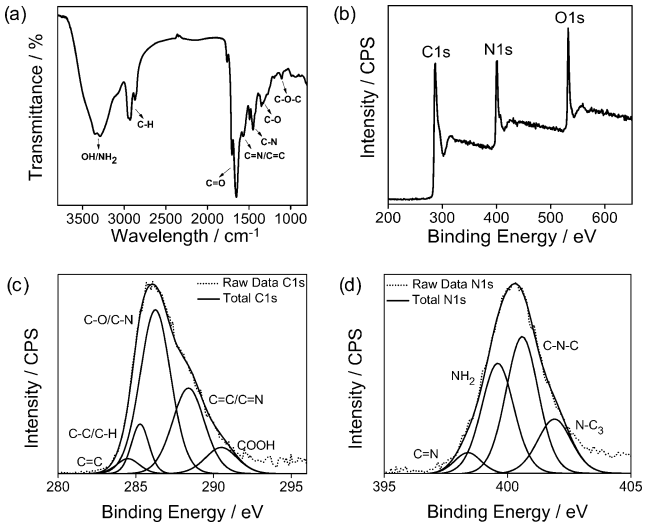

Figure 3. a) FTIR spectrum of ap-NCNDs; b) XPS survey of ap-NCNDs; c) deconvoluted C1s spectrum of ap-NCNDs; d) deconvoluted N1s spectrum of ap-NCNDs.

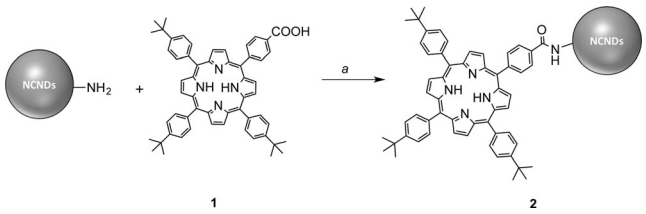

Scheme 1. Synthesis of the NCNDs-porphyrin conjugate **2**. Reagents and conditions: a) EDC, NHS, DMF, RT, overnight.

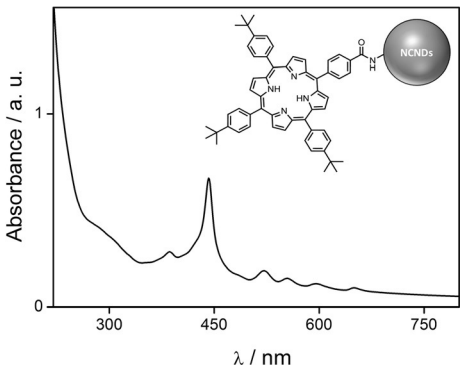

Figure 4. UV/Vis absorption spectrum of the NCNDs-porphyrin conjugate **2** in water.

and from the UV/Vis spectrum (Figure 4) the absorption of both NCNDs and porphyrin can be easily identified. Thus, the coupling of porphyrin to NCNDs results in its solubility in water media that could be not achieved for the porphyrin alone. Therefore, NCNDs can be used as water soluble carriers.

The cyclic voltammogram of ap-NCNDs shows two irreversible peaks corresponding to the oxidation (+1.14 V vs. SCE) and reduction (−2.52 V vs. SCE) of amines (Figure S23). The high current in oxidation and the steep slope of the peak are remarkable, demonstrating that a high quantity of amino groups on the surface can be easily oxidized.

The XPS survey spectra for NCNDs **1**, NCNDs **2**, and NCNDs **3** and spectra of C1s and N1s are reported in Figures S24 and S25, while the XPS data for NCNDs **1**–**3**, along with that of ap-NCNDs are collected in Table 1.

Table 1: Percentage of C, N, and O atoms in ap-NCNDs and NCNDs **1**–**3**, as determined by XPS measurements.

	ap-NCNDs	NCNDs **1**	NCNDs **2**	NCNDs **3**
C%	68.0	65.9	68.7	63.9
C=C	3.4	21.7	4.1	15.8
C–C	8.7	25.1	25.6	6.4
C-O C-N	50.1	28.2	53.0	56.2
C=O C=N	28.7	24.9	14.7	21.6
COOH	9.1	–	2.5	–
N%	16.1	11.1	9.0	7.0
C=N	5.4	–	10.6	–
NH_2	35.0	40.6	20.4	17.8
C-N-C	43.1	46.7	57.1	70.7
N-C3	16.5	12.7	11.9	11.4
O%	15.9	23.0	22.3	29.0

The results show that all of the NCNDs contain multiple oxygen and nitrogen functional groups on the particle surface, but with different contents, consistent with the FT-IR measurements.

The functional groups located at the surface of NCNDs act as a passivation layer, which improves their hydrophilicity and stability in aqueous systems, as well as their efficient photoluminescence properties.[6]

The aqueous solutions (0.5 mg mL^{-1}) of ap-NCNDs appeared yellow in daylight and remained stable for several weeks, with no change in their spectral features.

Upon excitation under a 365 nm UV lamp, ap-NCNDs emit with strong blue luminescence, while the UV/Vis spectrum of ap-NCNDs show an absorption band at 286 nm, ascribed to the π-π* transition of the conjugated C=C units from the carbon core (Figure 5a).[1,5]

Fluorescence (FL) is one of the most fascinating features of CNDs. Spectrally broad FL emission with excitation wavelength dependence is a common phenomenon observed in CNDs.[6,31] CNDs produce multi-fluorescence colors under different excitation wavelengths, and this behavior may arise not only from particles of different size but also from a distribution of different emissive domains on each carbon dot.

This property implies that the emission of CNDs can be tuned by changing the excitation wavelength since the emission arises from different surface emissive traps.

The luminescence properties of the ap-NCNDs have been explored. A broad emission peak at 356 nm is observed when the sample is excited at the optimal excitation wavelength (300 nm, Figure 5b). The fluorescence peaks shift from 356 nm to 474 nm when the excitation wavelength changes from 300 to 420 nm and the fluorescence intensity decreased as the peak red shifts. The many kinds of functional groups

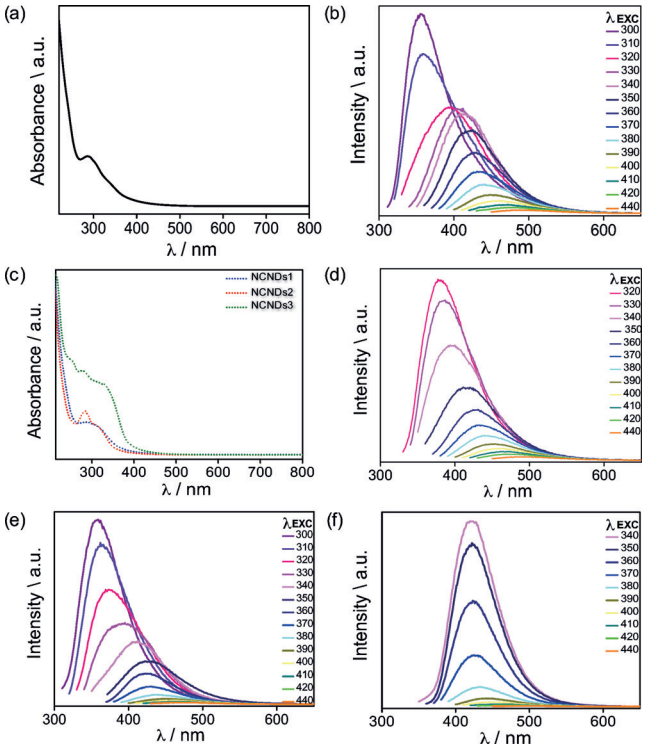

Figure 5. a) UV/Vis absorption spectrum of ap-NCNDs in water; b) FL spectra of ap-NCNDs in water (298 K) at different excitation wavelengths; c) UV/Vis absorption spectra of NCNDs **1**–**3** in water; d–f) FL spectra of NCNDs **1**–**3** in water (298 K) at different excitation wavelengths.

present on the surface of ap-NCNDs have different surface state energy levels, which result in a series of emissive traps that dominate the emission at different excitation wavelengths and explain the excitation wavelength-dependent phenomenon of ap-NCNDs. The fluorescence quantum yield (FLQY) was found to be 0.17, using a reported procedure and quinine sulphate as the reference (Supporting Information).[32,33]

As expected, the size and functional groups affect the optical properties. Figure 5c shows NCNDs **1**–**3** UV/Vis absorption spectra. NCNDs **1** have an absorption peak located at 315 nm, NCNDs **2** have two peaks at 285 and 315 nm, and NCNDs **3** have three peaks at 253, 278, and 328 nm. These peaks are most probably related to the electron transitions from π (or n) to π* of C=C and C=O.[1,5]

Typically, as the particles become smaller, the luminescence energies are blue shifted to higher energies.[34] However, the FL mechanism of CNDs is affected also by the zigzag edge sites and defects effect. Therefore, size-independent FL could be also observed because the surface state emission can play a predominant role in the FL properties.[35]

NCNDs **1**–**2** show clear excitation-dependent emission spectra, whereas NCNDs **3** exhibit an almost excitation-independent behavior. Each sample has its optimal emission for a characteristic excitation wavelength, revealing the presence of different energy levels corresponding to the maximum transition probability (Figure 5d–f). The surface of NCNDs significantly affects the FL properties because it determines the trapping of excitons under excitation. Therefore, the radiative recombination of those surface-trapped excitons leads to FL with the corresponding energy. NCNDs **1**, NCNDs **2**, and NCNDs **3** exhibited their most intense emission at 380 nm (excitation at 320 nm), 357 nm (excitation at 300 nm), 421 nm (excitation at 340 nm), respectively. The FLQYs of NCNDs **1**, NCNDs **2**, and NCNDs **3** were 0.07, 0.31, and 0.46. To the best of our knowledge, the latter is among the highest FLQY values so far reported for CNDs.[4] Figure 6 clearly shows the increased emitted blue luminescence from NCNDs **1** to NCNDs **3** upon excitation under a 365 nm UV lamp.

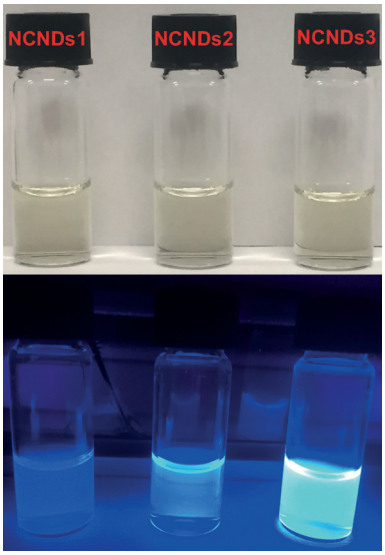

Figure 6. Photographs of NCNDs **1**, NCNDs **2**, and NCNDs **3** in daylight (top) and under UV light (365 nm) illumination (bottom).

As reported in Table 1, NCNDs **1**–**3** have similar functional groups and nitrogen content. The QYs increase with the reduced amount of amino groups, with NCNDs **3** having the highest degree of surface oxidation, resulting in more surface defects, which can trap more excitons leading to higher FL quantum yield.[36]

In summary, we have described a straightforward, simple and controllable method to prepare NCNDs under microwave irradiation. Using this approach, NCNDs could be obtained within three minutes without the need of sophisticated equipment or additional surface passivation. We have reported a general method for the separation of three fractions of NCNDs with different size and properties by low-pressure gel permeation chromatography. These NCNDs are narrowly distributed in size, and their abundant surface traps and functional groups endowed them with tunable fluorescent emission, bright luminescence (quantum yield as high as 0.46), and excellent solubility in water and in common polar organic solvents. We have demonstrated that these NCNDs can be easily functionalized and, more importantly, that they can be used as water-soluble carriers. Moreover, we have shown that the fluorescence strongly depends on the surface states of the NCNDs because their optical properties

are affected by the competition among different emission centers and traps. This work provides a route to size- and surface-controllable NCNDs. Their superior optical properties, coupled with their low cost and ease of labeling, should enable their use in numerous applications, which are currently underway in our laboratory.

Acknowledgements

Financial support from the University of Trieste, Consorzio Interuniversitario Nazionale per la Scienza e Tecnologia dei Materiali (INSTM), Ministero dell'Università e della Ricerca (MIUR) (FIRB prot. RBAP11C58Y and Cofin. Prot. 2010N3T9M4) and the European Commission (FP7/2007-2013 under grant agreement number 310651, SACS project) are gratefully acknowledged. We thank Prof. R. Noto and Dr. S. Riela (University of Palermo), Prof. L. De Cola and Ms. S. Carrara (University of Strasbourg), and Prof. S. Antoniutti (University of Venezia) for their great help and support.

Keywords: carbon nanodots · nanoparticles · nanostructures · self-assembly

How to cite: *Angew. Chem. Int. Ed.* **2016**, *55*, 2107–2112
Angew. Chem. **2016**, *128*, 2147–2152

[1] Y.-P. Sun, B. Zhou, Y. Lin, W. Wang, K. A. S. Fernando, P. Pathak, M. J. Meziani, B. A. Harruff, X. Wang, H. Wang, et al., *J. Am. Chem. Soc.* **2006**, *128*, 7756–7757.
[2] X. Xu, R. Ray, Y. Gu, H. J. Ploehn, L. Gearheart, K. Raker, W. A. Scrivens, *J. Am. Chem. Soc.* **2004**, *126*, 12736–12737.
[3] V. Georgakilas, J. A. Perman, J. Tucek, R. Zboril, *Chem. Rev.* **2015**, *115*, 4744–4822.
[4] S. Y. Lim, W. Shen, Z. Gao, *Chem. Soc. Rev.* **2015**, *44*, 362–381.
[5] P. Roy, P.-C. Chen, A. P. Periasamy, Y.-N. Chen, H.-T. Chang, *Mater. Today* **2015**, *18*, 447–458.
[6] S. N. Baker, G. A. Baker, *Angew. Chem. Int. Ed.* **2010**, *49*, 6726–6744; *Angew. Chem.* **2010**, *122*, 6876–6896.
[7] S.-T. Yang, L. Cao, P. G. Luo, F. Lu, X. Wang, H. Wang, M. J. Meziani, Y. Liu, G. Qi, Y.-P. Sun, *J. Am. Chem. Soc.* **2009**, *131*, 11308–11309.
[8] L. Cao, X. Wang, M. J. Meziani, F. Lu, H. Wang, P. G. Luo, Y. Lin, B. A. Harruff, L. M. Veca, D. Murray, et al., *J. Am. Chem. Soc.* **2007**, *129*, 11318–11319.
[9] J. Tang, B. Kong, H. Wu, M. Xu, Y. Wang, Y. Wang, D. Zhao, G. Zheng, *Adv. Mater.* **2013**, *25*, 6569–6574.
[10] M. Zheng, S. Liu, J. Li, D. Qu, H. Zhao, X. Guan, X. Hu, Z. Xie, X. Jing, Z. Sun, *Adv. Mater.* **2014**, *26*, 3554–3560.
[11] J. Lei, L. Yang, D. Lu, X. Yan, C. Cheng, Y. Liu, L. Wang, J. Zhang, *Adv. Opt. Mater.* **2015**, *3*, 57–63.
[12] H. Li, X. He, Z. Kang, H. Huang, Y. Liu, J. Liu, S. Lian, C. H. A. Tsang, X. Yang, S.-T. Lee, *Angew. Chem. Int. Ed.* **2010**, *49*, 4430–4434; *Angew. Chem.* **2010**, *122*, 4532–4536.
[13] F. Wang, Y. Chen, C. Liu, D. Ma, *Chem. Commun.* **2011**, *47*, 3502–3504.
[14] X. Zhang, Y. Zhang, Y. Wang, S. Kalytchuk, S. V. Kershaw, Y. Wang, P. Wang, T. Zhang, Y. Zhao, H. Zhang, et al., *ACS Nano* **2013**, *7*, 11234–11241.
[15] X. Yu, J. Liu, Y. Yu, S. Zuo, B. Li, *Carbon* **2014**, *68*, 718–724.
[16] A. Zhao, Z. Chen, C. Zhao, N. Gao, J. Ren, X. Qu, *Carbon* **2015**, *85*, 309–327.
[17] P. G. Luo, F. Yang, S.-T. Yang, S. K. Sonkar, L. Yang, J. J. Broglie, Y. Liu, Y.-P. Sun, *RSC Adv.* **2014**, *4*, 10791.
[18] H. Zheng, Q. Wang, Y. Long, H. Zhang, X. Huang, R. Zhu, *Chem. Commun.* **2011**, *47*, 10650–10652.
[19] Y. Dong, H. Pang, H. Bin Yang, C. Guo, J. Shao, Y. Chi, C. M. Li, T. Yu, *Angew. Chem. Int. Ed.* **2013**, *52*, 7800–7804; *Angew. Chem.* **2013**, *125*, 7954–7958.
[20] X. Chen, Q. Jin, L. Wu, C. Tung, X. Tang, *Angew. Chem. Int. Ed.* **2014**, *53*, 12542–12547; *Angew. Chem.* **2014**, *126*, 12750–12755.
[21] G. Sandeep Kumar, R. Roy, D. Sen, U. K. Ghorai, R. Thapa, N. Mazumder, S. Saha, K. K. Chattopadhyay, *Nanoscale* **2014**, *6*, 3384–3391.
[22] J. Moon, J. An, U. Sim, S.-P. Cho, J. H. Kang, C. Chung, J.-H. Seo, J. Lee, K. T. Nam, B. H. Hong, *Adv. Mater.* **2014**, *26*, 3501–3505.
[23] Y. Xu, M. Wu, Y. Liu, X.-Z. Feng, X.-B. Yin, X.-W. He, Y.-K. Zhang, *Chem. Eur. J.* **2013**, *19*, 2276–2283.
[24] J. Jiang, Y. He, S. Li, H. Cui, *Chem. Commun.* **2012**, *48*, 9634–9636.
[25] X. Zhai, P. Zhang, C. Liu, T. Bai, W. Li, L. Dai, W. Liu, *Chem. Commun.* **2012**, *48*, 7955–7957.
[26] H. Zhu, X. Wang, Y. Li, Z. Wang, F. Yang, X. Yang, *Chem. Commun.* **2009**, 5118–5120.
[27] S. Chandra, P. Das, S. Bag, D. Laha, P. Pramanik, *Nanoscale* **2011**, *3*, 1533–1540.
[28] D. Mazzier, M. Favaro, S. Agnoli, S. Silvestrini, G. Granozzi, M. Maggini, A. Moretto, *Chem. Commun.* **2014**, *50*, 6592–6595.
[29] Z. Yang, Z. Li, M. Xu, L. Zhang, J. Zhang, Y. Su, F. Gao, H. Wei, L. Zhang, *Nano-Micro Lett.* **2013**, *5*, 247–259.
[30] Y. Yang, J. Cui, M. Zheng, C. Hu, S. Tan, Y. Xiao, Q. Yang, Y. Liu, *Chem. Commun.* **2012**, *48*, 380–382.
[31] V. Strauss, J. T. Margraf, C. Dolle, B. Butz, T. J. Nacken, J. Walter, W. Bauer, W. Peukert, E. Spiecker, T. Clark, et al., *J. Am. Chem. Soc.* **2014**, *136*, 17308–17316.
[32] J. R. Lakowicz, *Principles of Fluorescence Spectroscopy*, 3rd ed., **2006**.
[33] C. Würth, M. Grabolle, J. Pauli, M. Spieles, U. Resch-Genger, *Nat. Protoc.* **2013**, *8*, 1535–1550.
[34] R. Ye, C. Xiang, J. Lin, Z. Peng, K. Huang, Z. Yan, N. P. Cook, E. L. G. Samuel, C.-C. Hwang, G. Ruan, et al., *Nat. Commun.* **2013**, *4*, 2943.
[35] L. Tang, R. Ji, X. Li, G. Bai, C. P. Liu, J. Hao, J. Lin, H. Jiang, K. S. Teng, Z. Yang, et al., *ACS Nano* **2014**, *8*, 6312–6320.
[36] S. Zhu, J. Zhang, X. Liu, B. Li, X. Wang, S. Tang, Q. Meng, Y. Li, C. Shi, R. Hu, et al., *RSC Adv.* **2012**, *2*, 2717–2720.

Received: November 1, 2015
Revised: December 3, 2015
Published online: January 6, 2016

